Acoustic radiation patterns of mating calls of the túngara frog (*Physalaemus pustuosus*): Implications for multiple receivers

Ximena E. Bernal[a] and Rachel A. Page[b]
Section of Integrative Biology, University of Texas at Austin, 1 University Station C0930, Austin, Texas 78712

Michael J. Ryan
Section of Integrative Biology, University of Texas at Austin, 1 University Station C0930, Austin, Texas 78712 and Smithsonian Tropical Research Institute, P.O. Box 0943-03092, Balboa Ancón, Republic of Panamá

Theodore F. Argo IV and Preston S. Wilson
Department of Mechanical Engineering and Applied Research Laboratories, University of Texas at Austin, P.O. Box 8029, Austin, Texas 78713-8029

(Received 22 November 2008; revised 30 July 2009; accepted 31 July 2009)

In order for a signal to be transmitted from a sender to a receiver, the receiver must be within the active space of the signal. If patterns of sound radiation are not omnidirectional, the position as well as the distance of the receiver relative to the sender is critical. In previous measurements of the horizontal directivity of mating calls of frogs, the signals were analyzed using peak or root-mean-square analysis and resulted in broadband directivities that ranged from negligible to a maximum of approximately 5 dB. Idealized laboratory measurements of the patterns of acoustic radiation of the mating calls of male túngara frogs (*Physalaemus pustulosus*), along axes relevant to three receivers in this communication network, female frogs in the horizontal plane, and frog-eating bats and blood-sucking flies above the ground, are reported. The highest sound pressure level was radiated directly above the frog, with a 6 dB reduction radiated along the horizontal direction. Band-limited directivities were significantly greater than broadband directivities, with a maximum directivity of 20 dB in the vertical plane for harmonics near 6 kHz. The implications with regard to mating and predator-prey interactions are discussed.
 [DOI: 10.1121/1.3212929]

PACS number(s): 43.80.Ka [MJO] Pages: 2757–2767

I. INTRODUCTION

In its simplest form, communication is a dyadic interaction between a signaler and a receiver in which the signal has some probabilistic influence on the behavior of the receiver.[1] For communication to proceed, the signal must be detected and perceived by the receiver; that is, the receiver must be within the active space of the signal. In acoustic communication, the size of the active space is dependent on the amplitude of the signal at the source, the patterns of radiation of the signal, and the sensitivity of the receiver. If patterns of sound radiation are not omnidirectional, the position of the receiver relative to the sender is critical. In many animal systems, the radiation of acoustic signals is directional, often with higher amplitude anterior to the sender with a bilaterally symmetric sound field around it.[2–5] Some species of frogs and toads produce nearly omnidirectional acoustic radiation in the horizontal plane while others have 5 dB or more of directivity.[6] In some species, such as the sage grouse, the directionality or beam pattern of the sound is more pronounced.[7]

Not all communication is dyadic. In many systems animals send signals to more than one receiver within a social group of conspecifics. Quantifying directionality of the source is important to define the communication network. In many if not most acoustic communication systems, such as chorusing insects, frogs, and birds, the multiple conspecific receivers are often in the same plane and have similar thresholds for signal detection. Quite often, however, there are unintended receivers or "eavesdroppers."[8,9] These receivers attend to the same signals as do the conspecifics but for a different reason, they use the signals as acoustic beacons to lead them to potential prey or hosts. In a classic example, the mating calls of male field crickets attract both female crickets for mating and the fly *Ormia*, which locates the call of the cricket and deposits its larvae on the male. The larvae burrow into the male cricket and use him as a food source as they develop.[10] Heterospecifics that eavesdrop on the mating signals of their hosts or prey are widespread across taxonomic groups (e.g., gecko-cricket,[11] bat-katydid,[12] emblysoma fly-cicada,[13] orminiie fly-bushcricket,[14,15] heron-cricket,[16] opossum-frog,[17] and turtle-frog[18]). In cases

[a]Present address: Department of Biological Science, Texas Tech University, Box 43131 Lubbock, TX 79409.
[b]Present address: Sensory Ecology Group, Max Planck Institute for Ornithology, 82319 Seewiesen, Germany.

in which the signaler and the intended receiver communicate in the horizontal plane while the unintended receiver detects the signal in a vertical plane, the characteristics of the signal available to the different receivers may vary greatly. Thus, beaming patterns of the signal influence its effectiveness at attracting mates and the costs imposed by acoustically orienting predators and parasites. Although considerable attention has been devoted to signal adaptations that increase signal transmission through the environment,[19–21] the role of the beam pattern in signal evolution has been largely ignored.

In this study, patterns of acoustic radiation of mating calls of male túngara frogs (*Physalaemus pustulosus*) were measured. This neotropical frog is a well-known model organism for studies of vertebrate communication (see reviews in Refs. 22 and 23). Males produce acoustic signals, or mating calls, that are the primary cue females use to locate and assess males for mating. All calls contain a multi-harmonic frequency sweep, the whine. During the sweep, the first harmonic traverses frequencies from approximately 900 to 400 Hz in approximately 300 ms. The whine can be produced by itself or can be followed by 1–7 short, broadband bursts of sound, the chucks, each with a duration of about 45 ms.[24] The whine by itself, the simple call, is necessary and sufficient to elicit phonotactic responses from females, while the addition of chucks, which form complex calls, increases the attractiveness of the call to females. Males tend to produce simple calls when calling in isolation but escalate to complex calls in response to calls of other males. In this study, few males produced chucks, and, therefore, the chucks were omitted from the analysis.

The production of complex calls is favored by sexual selection because it increases the males' probability of mating. There are, however, two primary eavesdroppers in this system: the frog-eating bat *Trachops cirrhosus*[25] and the blood-sucking fly *Corethrella*,[26] both of which are attracted to the calls of male túngara frogs. Both eavesdroppers have call preferences similar to those of female túngara frogs; they are attracted to simple calls but prefer complex ones.[27] Both eavesdroppers approach the calling males from above while the female frogs approach the males in the horizontal plane.

The purpose of this study is to document in an idealized environment the patterns of acoustic radiation along axes relevant to the three known receivers in this communication network: the female frogs in the horizontal plane, and the frog-eating bats and blood-sucking flies above the ground. The purpose of this study is not to duplicate conditions in which frogs call in nature. In fact, there is no single calling condition because weather, topography, and intervening vegetation at calling sites all vary substantially across time and space. Instead, the purpose is to define a benchmark in which acoustic radiation is quantified precisely with variables eliminated, e.g., intervening vegetation, or controlled, e.g., topography, temperature, and humidity. This benchmark can then be used as a standard against which to assess radiation patterns in the wild.

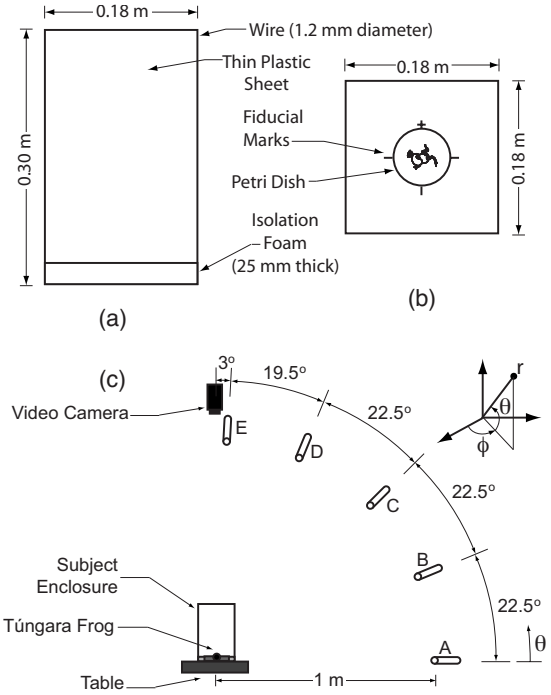

FIG. 1. Diagram of the subject enclosure. Panel (a) shows the side view and panel (b) shows the top view of the enclosure. A schematic (c) of the directivity microphone array is shown. All microphones were placed 1 m from the center of the petri dish. The angular coordinate system is also shown. The angles θ and ϕ are referred to as elevation and azimuth, respectively.

II. MATERIALS AND METHODS

A. Subjects

Ten male túngara frogs were tested from a breeding colony at the University of Texas at Austin, TX from December 8, 2006 to January 5, 2007. Colony frogs were maintained on an adjusted light/dark cycle such that dawn began at 02:00 and dusk began at 14:00. Males were tested from 18:00 to 01:00, during their active period. The mean mass of the males tested was 1.31 g, and the mean snout-vent length was 26.46 mm. These measurements are within the range of measurements of male frogs found in the wild.[22] After testing, the males were returned to the colony and marked using a toe-clipping system to avoid using the same individual more than once in the experiment.

To stimulate calling behavior, males were injected with 500 IU human chorionic gonadotropin (HCG) 24–48 h prior to testing. HCG has been shown to stimulate reproductive behavior in anurans.[28] HCG was dissolved in 0.9% saline solution and injected subcutaneously in a volume of 0.5 ml. In túngara frogs, HCG injection does not alter the characteristics of the call (M. Ryan, personal observation). All tests were licensed and approved by the University of Texas at Austin (IACUC Protocol No. 6041701).

Males were placed one at a time in a $18\times18\times30$ cm^3 enclosure depicted in Fig. 1. The walls of the enclosure consisted of transparent plastic film (thickness=0.0381 mm) loosely supported by 1.2 mm diameter wire. Such an enclosure was previously shown to be acoustically transparent to túngara frog calls.[29] In addition, the acoustic pressure level transmitted by a directional 38 kHz source was measured at

various angles from within the enclosure and compared to the level transmitted in absence of the enclosure. Variation among these measurements was less than 0.5 dB, which is small compared to the directional variation discussed in Sec. III and was thus ignored. The enclosure was open at the top, allowing for unobstructed view from above. The position of the frogs was tracked with a video camera positioned directly above. The base of the enclosure consisted of 25.5 mm thick foam, with a 6.7 cm diameter petri dish inset into the center. The petri dish was filled with water to afford the males an appropriate environment for calling. In nature, túngara frogs are found calling only in shallow water, and it is thought that water is necessary for full expansion of the vocal sac.[22]

The enclosure was positioned in the center of a 30×60 cm^2 table, which itself was placed at the center of a $3.62 \times 2.46 \times 2.20$ m^3 fully anechoic chamber. The table was used to mimic the acoustical effect of the water surface from which túngara frogs call. To waves incident in air, both water and the hard surface of a wood table appear acoustically rigid, and both are smooth and flat. The large walk-in anechoic chamber used in this work is located in the basement of its building, attached to the foundation. It is fully enclosed by an outer shell of solid concrete blocks and an inner shell, also made of solid concrete blocks. There is a 1 ft air gap separating the outer and inner shells on all sides and the inner shell is suspended on springs and dampers for isolation from low frequency structure-borne sound and vibration. Acoustic isolation doors on each shell allow access into the chamber. The inner walls, door, ceiling, and floor of the chamber are fully covered with 3 ft long sound-absorbent fiberglass wedges. The wedges are attached to the inside of the inner shell via a compliant mounting and are placed in groups of three. The orientation of the edges of each group of wedges alternates between horizontal and vertical between neighboring groups. A removable wire mesh platform is suspended above the floor-mounted wedges to allow users to walk into the chamber. Measurements provided by the manufacturer indicate that the noise floor of the chamber is 0–10 dB re 20 μPa, depending primarily on the traffic level on the street outside the building, and that free field conditions exist within the chamber at frequencies above 200 Hz.

The temperature in the entire chamber was controlled with a space heater to obtain temperatures appropriate for the frogs to call (approximately 26 °C). A room humidifier was used to increase the humidity of the air in the chamber, also to facilitate calling by the frogs. A relative humidity of 40%–50% was the maximum that could be achieved. The frog's natural environment usually has a higher humidity, but this humidity difference results in a negligible difference in acoustic propagation. The sound speed change is less than 0.3% for air at 50% and 100% relative humidities, at the experimental temperature,[30] and there is a maximum of 0.03 dB difference in attenuation along the experimental propagation path for this humidity difference.[31] The subjects acclimated for over 1 h inside the enclosure in the chamber before measurements began.

A recording of a túngara frog chorus was then broadcast from a small loudspeaker located approximately 1.5 m from the frog enclosure to evoke calling by the test male. Once the test male began calling in response to the chorus, the amplitude of the chorus playback was gradually reduced until the male called in silence. The spectral content, amplitude, and repetition rate of the calls recorded in the present experiment are typical of calls recorded in the natural environment.[22]

B. Measurement instrumentation

Calling behavior was recorded with a night vision video camera positioned 1 m above the frog enclosure. These data allowed us to determine the orientation and position of the frog within the enclosure for each recorded call. All trials were conducted in darkness, illuminated only by the infrared light on the video camera. Optomotor studies show that túngara frogs are not sensitive to light in the infrared (X. Bernal and M. J. Ryan, unpublished data). The frog's orientation relative to the microphone array was determined by measuring the angle between the centerline connecting the frog's snout to the frog's vent and orthogonal tape marks on the foam base that were aligned with the microphone array.

Wide-bandwidth acoustic pressure recordings (10 Hz–51.4 kHz) of five frogs were obtained with a GRAS model 40BF free-field microphone positioned 0.63 m from the center of the petri dish. Some frogs produce calls in the ultrasonic range,[32] thus measurements were made in this frequency range to document the presence or absence of these frequencies in this species. The microphone was supported by a tripod-style microphone stand and was calibrated by the manufacturer. Its response was flat within ± 1.5 dB from 10 Hz to 50 kHz, and flat within ± 3 dB from 50 to 100 kHz. The microphone cartridge was connected to a GRAS type 26 preamplifier that possessed a flat (± 0.2 dB) bandwidth from 2 Hz to 200 kHz. The signals were digitized with a personal computer based data-acquisition board and a sampling rate of 102.8 kHz.

Audio-band acoustic pressure recordings (10 Hz–22.0 kHz) of five different frogs were obtained using five Sennheiser model ME66 audio-bandwidth microphones placed 1 m from the center of the petri dish in a plane perpendicular to the plane of the table, as shown in Fig. 1(c). The microphones at 0°, 22.5°, and 45° were placed in tripod-style microphone stands and the microphones at 67.5° and 87° were suspended using thin woolen string. The five Sennheiser microphones were calibrated by comparison with one of the GRAS microphones to within 0.2 dB of the GRAS response, which is significantly less than the directivity observed in the measured beam patterns reported in this work. The signals were recorded with a Racal Storeplex multichannel digital tape deck with a 96 dB dynamic range, using a sampling rate of 45.5 kHz. In-line impedance-matching microphone transformers were used to connect the balanced low-impedance microphones to the high-impedance, ground-referenced single-ended inputs on the tape deck. The microphone signals were played from tape and digitized with a data-acquisition system (also 96 dB dynamic range) running on a desktop computer.

C. Signal processing

Signal processing of the ultrasonic bandwidth data consisted of calculating fast Fourier transforms (FFTs) and spectrograms using commercially available signal processing software. For the audio-bandwidth data, commercially available signal processing software was also used to perform the following operations. The remaining discussion in this section applies only to the audio band data. Each channel was detrended to remove any dc-voltage bias. Each frog produced multiple calls in succession; therefore, time gates were applied to isolate single calls. The maximum frequency was typically less than 10 kHz; hence the data were downsampled to 22 kHz. The broadband sound pressure levels (SPLs) were computed for each channel. These SPLs were referenced to the maximum SPL received for that call. The broadband directivity was visualized by plotting on a polar plot the SPL of each channel as a function of the angle at which it was recorded.

Spectrograms were then computed via the short time Fourier transform. The calls were time gated into blocks 512 points in length with a 92.8% overlap (475 points) with the previous block. A 500-point Kaiser window with a beta value of 5 was applied to each block. A 2048-point FFT operated upon each windowed block in succession to produce a spectrogram.

Frequency-dependent directivity for each audio-band call was determined at a particular time t_0 near the beginning of the call, where the highest frequencies were found and where subharmonics were not present, by extracting the FFT at t_0 within the spectrogram. The relationship among the peak frequencies found within the FFT was examined to determine the harmonic structure of the call. Each channel's FFT contained a series of harmonics, the magnitudes of which were extracted using a peak-finding algorithm. The magnitude of each peak for each channel was converted to decibels normalized by the maximum SPL at that peak. Directivity patterns were constructed from the normalized SPLs for each harmonic. The number of harmonics at time t_0 in most calls received at most directions varied between 6 and 8, although 9 harmonics were visible in some signals.

III. RESULTS AND DISCUSSION

Of the ten males tested, five were recorded with the wide-bandwidth GRAS microphone to investigate high-frequency call components, and five were recorded with the audio-frequency-range Sennheiser microphone array to investigate beaming patterns. A total of 66 calls from five males were recorded with the wide-bandwidth GRAS microphone. The spectrogram of a typical call recorded with the wide-bandwidth system is shown in Fig. 2(a). The maximum frequency component that appears above the noise floor is at about 11.5 kHz. Individual FFTs from several times within the spectrogram are shown in Fig. 2(b). The thick black spectrum is close to the noise floor, from a quiet time past the end of the call. The three other spectra are from near the beginning of the call. Peaks that are lower in frequency than the peak labeled (α) are persistent over time. Peak (β) appears by itself. The thin black spectrum and the blue spectrum do not have corresponding peaks at this frequency. The peaks that are higher in frequency than (β) do not persist over time. Therefore, we conclude that the highest frequency that appears in the call is about 11.5 kHz. None of the remaining 65 calls that were recorded with the wideband system contained higher frequency content above the noise floor. This result is consistent with the observation of increasing attenuation above a few kilohertz in the frog's natural environment due to interaction with vegetation.[33]

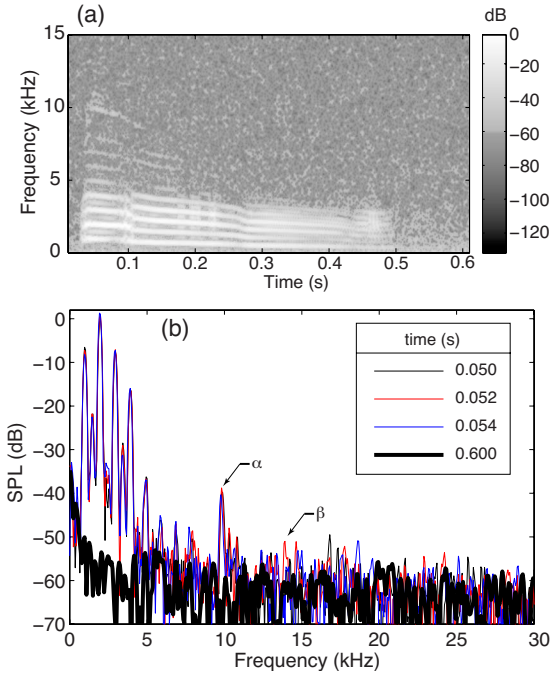

FIG. 2. (Color online) A spectrogram of a typical call recorded with the wide-bandwidth system is shown in (a). The highest persistent frequency component that appears above the noise occurs at 11.5 kHz. FFTs are shown in (b) from four times within the spectrogram of (a). The thick black spectrum is close to the noise floor, past the end of the call. The three remaining spectra are from near the beginning of the call. Peaks lower in frequency than the peak labeled (α) are persistent over time and correspond to the call. Peak (β) appears by itself. The thin black spectrum and the blue spectrum do not have corresponding peaks at this frequency. Peaks higher in frequency than (β) are not persistent over time but vary randomly; hence they are considered noise.

The remainder of the results reported here were obtained with the audio-frequency-range Sennheiser microphone array. Approximately 140 calls from five males were analyzed. A typical call is shown in Fig. 3(a). The waveforms were recorded at each of the five azimuthal angles given in Fig. 1(c). Microphone E is directly above the frog and microphone A is on ground level. A high-amplitude burst is visible at the onset of each waveform, followed by a decay; yet each waveform has a different envelope. For example, at 0.225 s there is a pronounced amplitude reduction in the high angle recordings (C, D, and E) and relatively less amplitude reduction in the low-angle recordings (A and B). In general, signal amplitude is retained at larger angles for a greater amount of time than at lower angles.

The broadband directivity of the call is shown in Fig. 3(b). The SPL of the waveform recorded at the ith angle was calculated with

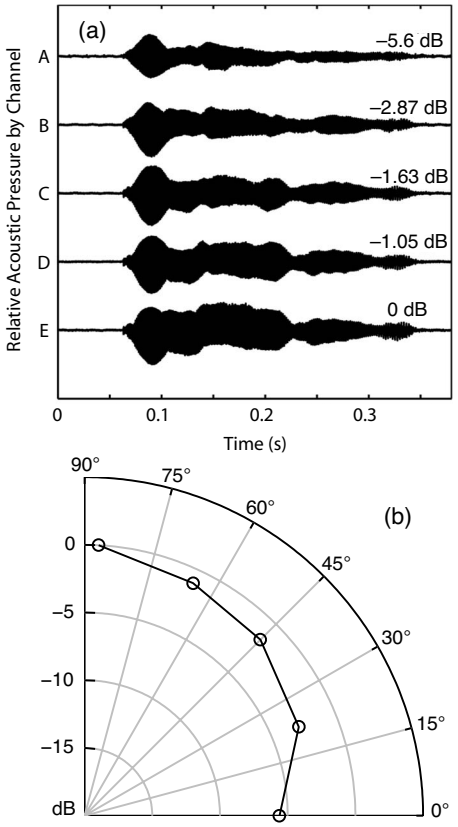

FIG. 3. Time waveforms of a typical túngara frog call recorded with the microphone array are shown in (a). The SPL, relative to the root-mean-square pressure recorded at microphone E (directly above the frog), is calculated for each channel. The broadband directivity in elevation plane θ is presented in (b), using the SPLs shown in (a).

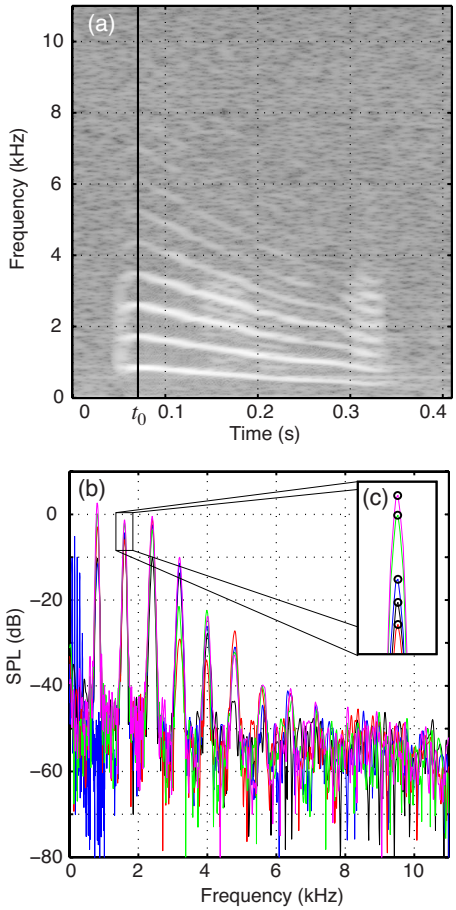

FIG. 4. (Color online) In this spectrogram (a) of a typical call, lighter shades of gray indicate higher amplitude. The time that corresponds to the highest frequency is indicated by the vertical line, at approximately 0.075 s. The FFTs at that time and all angles are shown in (b). At frequencies below 3 kHz peaks rise up to 50 dB above the noise, whereas at frequencies approaching 8 kHz the peaks become indistinguishable from the noise. In (c), the relative amplitude received at different elevation angles θ is shown for the second harmonic. These narrowband SPLs are presented (in Fig. 5) in the form of directivity plots for each harmonic, and for various azimuthal angles ϕ using calls from the same frog. The data in Fig. 5 were all taken at times within the call that corresponded to the highest frequency, as illustrated by the solid line at t_0 in Fig. 4(a).

$$\mathrm{SPL}_i = 20 \log_{10}\left[\frac{p_{\mathrm{rms},i}}{p_{\mathrm{rms,E}}}\right] (\mathrm{dB}), \tag{1}$$

where $p_{\mathrm{rms},i}$ is the rms pressure of the waveform recorded at the ith angle, $p_{\mathrm{rms,E}}$ is the rms pressure of highest amplitude waveform (microphone E), and the units are decibels. The highest SPL was radiated directly above the frog and the SPL is reduced at each angle until there is about a 6 dB reduction radiated along the horizontal direction.

Narrow-band directivity was also investigated. A spectrogram of signal E from Fig. 3(a) is shown in Fig. 4(a), where the call is seen to consist of a downward-sweeping chirp. At any given time, the call is composed of a series of harmonics, and the fundamental frequency decreases as time increases. This characteristic pattern of harmonics is shown in Fig. 4(b), for time t_0 indicated by the black vertical line in Fig. 4(a), but the spectra recorded at all five angles are shown. A close-up of the peaks associated with the second harmonic is shown in the inset, Fig. 4(c), where it can be seen that the narrowband amplitude received at each angle is different, and hence there is narrowband directivity, in addition to the broadband directivity already illustrated. Beam patterns are formed using these data in Figs. 5 and 6. The fundamental frequency of the calls in the dataset varied by at most a few percent with individual and from call-to-call in the same individual. Because of this variation, it was convenient to compare narrowband levels as a function of the harmonic number, instead of comparing them directly as a function of frequency.

Nonlinear phenomena are exhibited in the recorded calls. Subharmonics are visible in both the spectrograms and FFTs shown in Figs. 2 and 4. There are also frequency jumps in Fig. 2(a) located at about 0.1 s and just before 0.3 s. Such nonlinear features are common in other species' vocal production mechanisms[34] and calls that contain subharmonics have been documented for the túngara frog.[24] In túngara, these nonlinear features appear to be caused by nonlinear mechanical dynamics of the frog's vocal production mechanism. Specifically, a fibrous mass attached to the vocal folds that can undergo impact oscillation at a sufficiently high excitation level appears to be responsible for the presence of subharmonics in the portion of the call known as the chuck.[24] Subharmonic generation by impact oscillation (also known as clapping or impact nonlinearity) has been documented in many dynamic systems.[35–37]

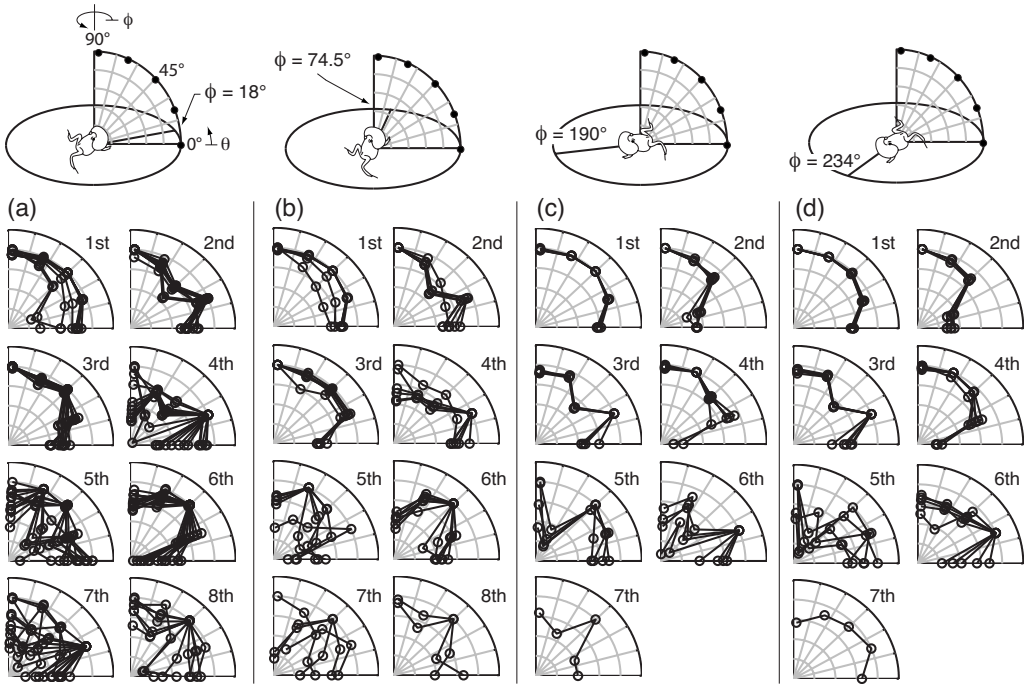

FIG. 5. Narrowband elevation directivity plots for a single frog at several azimuth angles are shown. Thirteen calls recorded at ϕ=18° are shown in (a). Six calls at ϕ=74.5° are shown in (b). Four calls at ϕ=190° are shown in (c). Five calls at ϕ=234° are shown in (d).

Despite these nonlinear phenomena, nonlinear acoustic propagation does not play a role in this work. The SPL of typical túngara frog calls (about 75–85 dB re 20 μPa),[22] and the propagation distance in this work (1 m) indicates that the acoustic propagation is linear. Nonlinear acoustic propagation effects only become important at higher amplitudes and for greater propagation distances, for example, 120 dB re 20 μPa and 100 m, as shown in Fig. 16.3.1 of Ref. 38. We therefore conclude that the sound radiation from the frog, the subsequent propagation, and call directivity are due to linear acoustic diffraction and are not effected by the source production mechanism's nonlinearity.

Directivity in the calls of one individual is illustrated for each harmonic at each of four azimuthal angles in Fig. 5. Beam patterns for several calls are shown in each frame where available. The data clearly display two characteristics. There is significant directivity in many of the harmonics, and there is significant variability from call-to-call, across different azimuthal angles and across different harmonics. The first harmonic generally mimics the broadband directivity of Fig. 3(b), with the main beam pointing directly above the frog, but in two calls in the first harmonic frame in Fig. 5(a), a dipole pattern is present. At higher harmonics, however, fairly strong beams appear, as in the sixth harmonic of Figs. 5(a) and 5(b), where the beam points at 45° above the horizon, as much as 20 dB higher in amplitude than signals oriented along the horizon at 0°. There is a large amount of call-to-call variability in some harmonics, the seventh har-

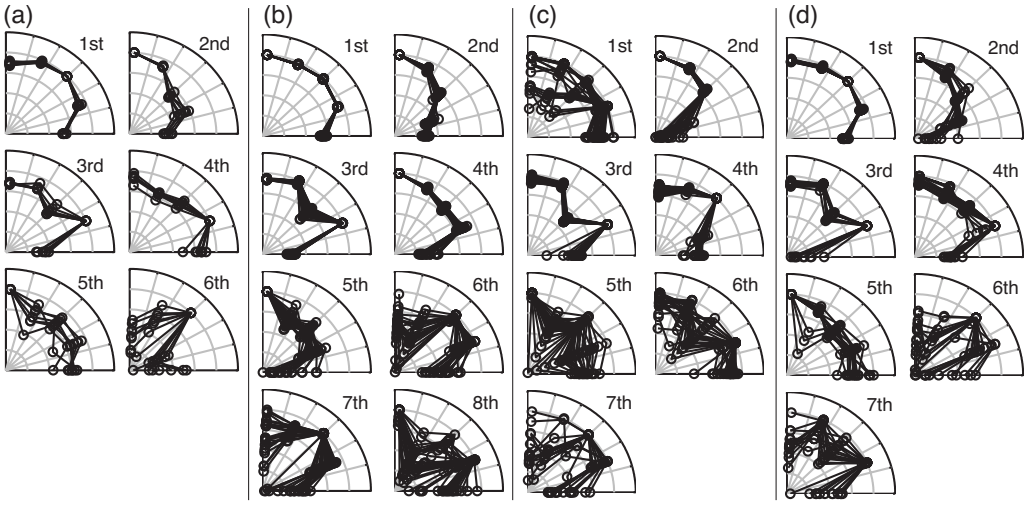

FIG. 6. Narrowband elevation directivity exhibited by four frogs at various azimuth angles is shown. Six calls by Frog 18 at ϕ=177° are shown in (a). Nineteen calls by Frog 19 at ϕ=121° are shown in (b). Twenty-five calls at ϕ=86° are shown in (c). Thirteen calls at ϕ=135° are shown in (d).

monic of Fig. 5(a), for example, while at the same time the third harmonic of Fig. 5(a) shows significantly less variability.

It is also interesting to consider the variability of the beam pattern at a particular harmonic as a function of azimuthal angle. Comparing the third and fourth harmonics in Figs. 5(a) and 5(b), to those in Figs. 5(c) and 5(d) reveals that, in each case, the patterns are different from front to back. For example, in Figs. 5(a) and 5(b), the third harmonic has a peak near 45°, which points up in the anterior direction, but in Figs. 5(c) and 5(d), there is a local minimum at 45°, in the posterior direction. The beams are reversed for the fourth harmonic, where a local minimum occurs in the anterior direction [Figs. 5(a) and 5(b)] and the directivity is relatively flat at 45° in the posterior direction [Figs. 5(c) and 5(d)]. Despite the variability, robust directivity clearly exists on average. The calls could be perceived differently to a listener depending on the relative position. This directivity could play a discrimination role for both intended and unintended listeners. Finally, when taken as a whole using the broadband directivity as a measure [Fig. 3(b)], more energy is directed upward, where the unintended listeners reside—the predators and parasites.[25,26] Relatively less energy is directed along the horizontal plane, where the intended listeners, the females, reside. This condition yields asymmetry between the costs and benefits associated with the túngara frog mating call.

The intention of this work is to illustrate the presence of directivity and variability in túngara calls. This work does not attempt to provide a species-wide generalized description of the call, nor to fully explain the ramifications of the directivity. Nonetheless, the results shown in Fig. 5 for a single individual are typical of the calls made by other males at other azimuthal angles, as illustrated in Fig. 6. At the current stage, there are not enough data from any one individual to fully populate the azimuthal angle parameter space, and not enough data from different individuals to calculate global mean beam patterns at even one angle. The current data do support the two main points mentioned previously: There is significant directivity in túngara frog calls, and the directivity exhibits significant variability from call-to-call, from harmonic-to-harmonic, and from individual-to-individual.

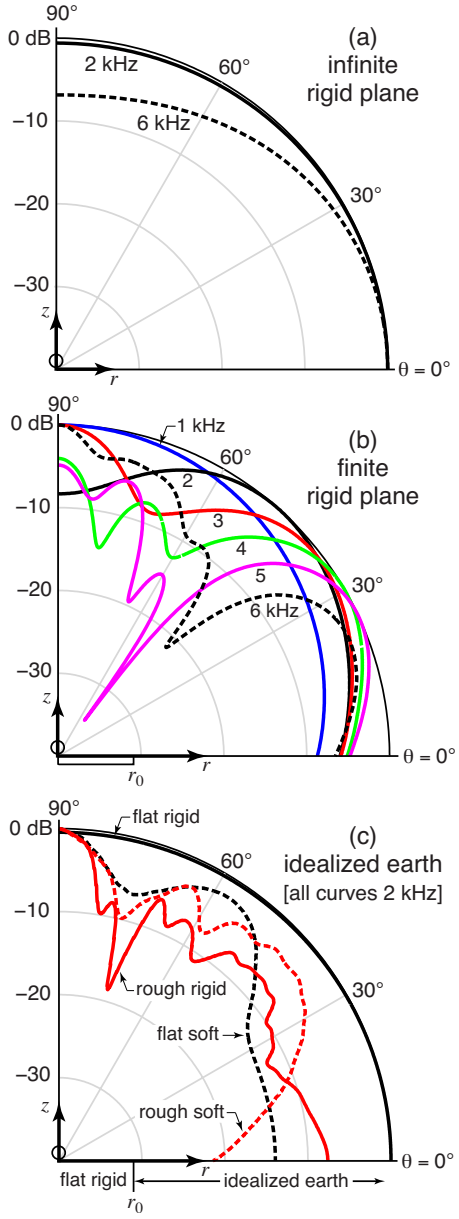

FIG. 7. (Color online) Model geometry and the results of directivity calculations are shown. The source location is indicated by the open circle at $r=0$ and $z=1$ cm. The directivity of a simple source above a rigid plane of infinite extent is shown in (a). The infinite plane lies along the r-axis and is perpendicular to the z-axis. Directivity at 2 and 6 kHz is shown. Directivity due to a finite-sized rigid reflecting plane is shown in (b) for a range of frequencies. The extent of the reflector is indicated by r_0. Directivities due to various representations of an idealized natural environment are shown in (c). A flat rigid reflector resides along the r-axis with radius r_0. Beyond r_0, four different realizations are shown: a continuation of the flat rigid reflector, a flat soft layer, a rough rigid layer, and a rough soft layer. Additional details are in the text.

IV. MODELING OF RADIATION PATTERNS

Several mathematical and numerical models were developed and used to interpret the radiation patterns presented in Sec. III. The goal of this modeling effort was to illuminate the leading order parameters that govern some of the features observed in the vertical plane directivity. The modeling was not intended to explain fine structure or details of either vertical or horizontal directivity. These models are based on the assumption that the acoustically active part of the frog is small compared to the acoustic wavelength for the frequencies discussed here, and hence the frog was modeled as a simple source. All simple sources produce the same acoustic field, that of a uniformly pulsating sphere, regardless of their shape.[38] The vocal sac of the túngara frog is the primary source of acoustic radiation[39–43] and it is approximately spheroidal in shape, with a nominal width during the whine of about 2 cm, for calls without chucks.[41] At the lowest frequencies analyzed in this work, about 1 kHz, the wavelength is about 34 cm, or 17 times the width of the vocal sac; hence the simple source assumption is well-justified. At the highest frequencies analyzed in this work, near 6 kHz, the wavelength is about 5.7 cm, or 2.85 times the width of the vocal sac, and the simple source assumption is less well-justified. The vocal sac can be larger, about 2.5 cm for calls with strong chucks,[41] which were not observed in this work. The effective volume of the vocal sac during the whine of a call

with no chuck is about 3000 mm^3 which yields an effective spherical radius of about 1 cm. Based on these dimensions and the simple source assumption, the frog's acoustic radiator was modeled as a uniformly pulsating sphere of radius 1 cm.

The túngara frog always calls in shallow water, often in small pools, puddles, or near the edge of ponds, with its vocal sac mostly above the surface of the water.[22] The acoustic ramification is that water, despite being fluid, appears as a nearly perfect rigid acoustic reflector to waves incident in air[38] and its surface is smooth and flat. Further, these small pools or pond edges provide a finite-sized, flat, rigid reflecting surface, bounded by soil and vegetation, which has acoustically soft surface properties. A wide variety of earth surfaces, from grassland, to cultivated earth, to layered forest floors exhibit similar acoustic properties, when subjected to transient incident acoustic pulses from above, with measured specific acoustic impedances that range from about eight times that of air at 1 kHz, to about two times that of air at 10 kHz.[44] The petri dish and table used in this work were intended to provide an idealized finite sized rigid reflecting plane, bounded by acoustically soft material, the air surrounding the table.

The models presented below demonstrate that the basic features of the observed radiation patterns are due to the frog behaving acoustically as a small pulsating sphere (the vocal sac) calling just above a finite-sized acoustically rigid plane (the water surface in nature or the table in this work), surrounded by an acoustically soft surface (soil and vegetation in nature or air in this work).

A. Simple source above an infinite rigid plane

It is also useful to demonstrate that the observed directivity is dependent on the size of the acoustically rigid reflecting surface being finite, so the first model shown is that of a simple source over an *infinite* rigid plane. Using the image method, the directivity of the field produced by this configuration is[45]

$$H(\theta) = 20 \log_{10}[\cos(kh \sin \theta)] \text{ (dB)}, \quad (2)$$

where $k=2\pi f/c$, the distance of the source above the plane is h, and θ is the angle above horizontal. The sound speed in air was 343 m/s. Setting $h=1$ cm, which corresponds to the 1 cm radius source described above sitting directly on the plane, and letting $f=2$ kHz, which is about the frequency of the second harmonic in this work, one finds very little directivity, as shown in Fig. 7(a). Increasing the frequency to $f=6$ kHz, also shown in Fig. 7(a), results in about 7 dB difference between 0° and 90°, but the amplitude is lower directly above the source, which is the opposite of that observed in Sec. III, where the radiated level was greater directly above the frog for the first, second, and third harmonics. This result indicates that the source over a rigid plane is not sufficient to explain the observed directivity presented in Sec. III.

B. Simple source above a finite rigid plane bounded by air

The general nature of the experimental apparatus used in Sec. III was simulated using a commercially available finite element software package. A two-dimensional axisymmetric finite element solution of the Helmholtz equation was obtained in a hemispherical domain. The coordinate axes of this domain, the radial dimension r and the height above the reflecting plane z, and the simulation geometry are schematized in Fig. 7(b). The center of a spherical 1 cm radius source with a uniform prescribed velocity was placed at $r=0$ and $z=1$ cm, as shown with the open circle (size exaggerated). The source was placed above a rigid circular surface that resided in the r-plane at $z=0$, with radius $r_0=15$ cm and thickness 5 cm extending below the r-plane. The table used in the measurements in Sec. III had the same thickness and its short side occupied the same radial dimension as shown, but was rectangular, whereas the table in the simulation is circular when rotated about the axis of symmetry (z-axis). This concession was made to allow efficient computation via a two-dimensional axisymmetric domain. A rectangular table would have required a computationally-intensive three-dimensional domain. The remaining domain was filled with air (sound speed of 343 m/s and density of 1.2 kg/m^3) and terminated at $r=1$ m with an outgoing spherical radiation condition. The simulation domain occupied $+90° < \theta < -90°$, although only the upper quadrant is shown in Fig. 7.

The simulation was run at several frequencies ranging from 1 to 6 kHz and the SPL was calculated at $r=1$ m for $0 < \theta < +90°$. This mimics the location of the microphones used in the directivity measurements in Sec. III. The resulting beam patterns are shown in Fig. 7(b). All curves were normalized to 0 dB at the angle of their maximum value. At 1 kHz, the radiation is directed above, is about 8 dB greater than along the horizontal, and is very similar to the measured radiation pattern shown in Fig. 3(b) and Figs. 5(a)–5(d) for the first harmonic, which was also about 1 kHz. As the frequency increases, both simulation and measurement show that radiation can be directed both above and at other angles, and that localized minima can form. Compare this to the relatively omnidirectional radiation seen in Fig. 7(a) at 2 kHz for the source above an infinite rigid plane and the lack of localized minima at either frequency. A finite-sized rigid reflecting plane is required to achieve both upward vertical directivity and localized minima.

C. Simple source above a finite rigid plane bounded by idealized earthen surfaces

The following models were undertaken as steps toward simulating a few aspects of the frog's natural calling environment. The finite element simulation described in Sec. IV B was repeated with the following changes: All calculations reported in this section were for a frequency of 2 kHz. The domain was reduced to $0 < \theta < +90°$. The flat, rigid reflecting surface below the source was retained, but instead of bounding it with air, the material properties and surface roughness of the natural environment were simulated. To be-

gin though, a flat rigid plane extending the entire length of the r-axis was used to serve as a comparison to the analytical solution for the simple source above an infinite rigid plane discussed in Sec. IV A. The simulation result, labeled "flat rigid" in Fig. 7(c), agrees very well with the analytical solution shown in Fig. 7(a). This validates the finite element model and indicates that the model source radiating above a flat rigid infinite plane produces nearly omnidirectional radiation at 2 kHz.

Next, the effect of surface roughness was investigated. The flat rigid plane was retained out to $r_0=15$ cm, but for 15 cm$<r_0<1$ m, the flat rigid surface was replaced with a random rough rigid surface. The location of this surface is indicated in Fig. 7(c) by the label "idealized earth." The rms surface roughness was 1.6 cm. The resulting directivity is shown in Fig. 7(c) by the curve labeled "rough rigid." The level is now about 8 dB less along the horizontal than directly above.

The material below the rough surface (15 cm$<r_0<1$ m) was then given acoustically soft material properties to mimic soil and vegetation. A specific acoustic impedance four times that of air, $4z_{\text{air}}$, was used (sound speed of 686 m/s and density of 2.4 kg/m^3) as is appropriate for a variety of soils at 2 kHz,[44] and the layer was extended to $z=-10$ cm, bounded on the bottom by a rigid boundary. The resulting directivity is shown in Fig. 7(c) with the curve labeled "rough soft." Now, the level directed upward is 20 dB higher than along the horizontal.

Finally, the rigid flat surface along the r-axis was replaced, and a 2-cm-thick, flat layer of the same acoustically soft material, with a specific acoustic impedance four times that of air ($4z_{\text{air}}$, sound speed of 686 m/s, and density of 2.4 kg/m^3), was placed on top of it for 15 cm$<r_0<1$ m. The resulting radiation pattern is shown in Fig. 7(c) by the curve labeled "flat soft." Again, one finds more radiation directed up than along the horizontal, by about 13 dB.

The effect of the soft layer's specific acoustic impedance was also investigated by varying it from eight times the specific acoustic impedance of air, to twice that of air, which is the range of surface acoustic properties found in Ref. 44. The shapes of the radiation patterns were very similar to the flat soft curve in Fig. 7(c), but with slightly different absolute values. For example, the differences between upward and horizontal radiation levels were 12.7, 13, and 11.7 dB, as the layer's impedance was varied from $2z_{\text{air}}$, to $4z_{\text{air}}$, to $8z_{\text{air}}$, respectively. The upward directivity is not strongly dependent on the surface properties of the material surrounding the reflecting surface (the water surface in nature), within the expected range of values for a variety of soils.

The effect of the size of the reflecting surface was also investigated. Its radius is r_0, as shown in Fig. 7(c). The model was run for 5 cm$<r_0<50$ cm, which corresponds to a range of $0.29<r_0/\lambda<2.9$ when normalized by the acoustic wavelength in air. The layer's acoustic properties were set at four times the specific acoustic impedance of air (sound speed of 686 m/s and density of 2.4 kg/m^3). The shape of the directivity curves changed as r_0 changed, but upward directivity was present in all cases. The difference in level between upward and horizontal radiation ranged between 8 and 16 dB. For $r_0<\lambda$, the radiation pattern was dipole-like, with the maximum level radiated directly upward and the level monotonically decreasing toward the horizontal. For $r_0>\lambda$, the radiation patterns developed local maxima and minima, or lobes, and the number of lobes increased as r_0 increased. The difference between local maxima and minima were typically about 4 dB. These results indicate that the size of the reflecting surface (the pool of water in nature) affects the specifics of the radiation patterns, but it does not affect the presence of upward directivity, for reflecting surfaces that are up to 50 cm in radius. Upward directivity would eventually be lost for increasing r_0, as was shown for the infinite reflecting plane in Figs. 7(a) and 7(c), but recall that túngara frogs call from shallow water,[22] which limits either the size of the puddle or the distance of the frog from the edge of a large pond.

The models shown in this section indicate that a frog calling just above a finite-sized acoustically rigid surface, such as the table in the present measurements or a shallow pool of water in nature, bounded by an acoustically soft material or by a rough surface, will result in more acoustic energy being directed upward than along the horizontal. Since the túngara always calls in shallow water, either near the edge of a pond or in a small pool, it is likely that upward directivity will be found in nature, as was found in the idealized environment used in Sec. III. Since the geometry of the natural pools, and the acoustic properties of the various soils and vegetation that surround the pools are not constant, many details of the túngara radiation patterns found in nature will differ from place to place, but upward-directed radiation patterns will likely persist. The details of these radiation patterns would also depend on nonuniform surface vibration of the vocal sac and acoustic interaction with the parts of the frog's body that were not modeled here (head, legs, and body), hence potentially explaining the variability among individuals already observed in Sec. III.

V. CONCLUSIONS

Mating calls of male túngara frogs were recorded in an anechoic chamber using an ultrasound-bandwidth microphone and using an audio-bandwidth microphone array oriented to observe acoustic directivity in the elevation angle (the vertical plane). The frogs produced calls, frequency-modulated whines, which were found to contain narrowband harmonics. No coherent signal was observed in the whines above 11.5 kHz. Thus, unlike the calls of some frogs,[32] the whines of túngara frogs studied here do not contain information in the ultrasonic range. These calls do exhibit substantial broadband and narrowband directivity. There was broadband directivity, expressed through the relative SPL of the entire whine. Directly above the frog, the radiated SPL was typically 6 dB greater than that radiated near the horizontal direction. Narrowband directivity was also seen in many of the harmonics of the calls. Higher-frequency harmonics displayed an increased directivity, with a 10 to 20 dB difference in radiated amplitude between angular directions in the vertical plane. Some of the harmonics were directed 45° from the ground, while other harmonics projected directly above

the calling frog. Finally, there were considerable differences observed from call-to-call, for a single frog at a single azimuthal angle. There were also differences seen as a function of azimuthal angle and certainly differences among individuals.

The models presented in Sec. IV indicate that the directivity observed in the idealized laboratory environment is due to the presence of a finite-sized, acoustically-hard, flat reflecting surface underneath the calling frog. This surface was created by the table used in the measurements, and is acoustically similar to the water surface from which the frogs call in nature. If this surface is bounded by an acoustically soft material or by a rough surface, both of which are found in the frog's natural environment, then acoustic radiation will be directed upward at levels higher than along the horizontal. This acoustic radiation pattern presents an evolutionary dilemma for the calling frog. A male's mating success is dependent on projecting the mating call into the active space for females, which is the horizontal plane. Yet due to the call directivity observed in the laboratory and predicted to exist in nature, the active space is greater in the vertical plane where the bats and flies reside. Assuming these radiation patterns are called amplitude independent, any increase in call amplitude would asymmetrically increase the caller's exposure to eavesdroppers compared to mates, causing a relative increase in mortality risk for the caller. The directivity pattern of the sound field is one component of the frog's communication system that is subject to the competing costs and benefits of communicating. Thus understanding the biophysics of the communication system is necessary for a deeper understating of both its function and evolution.

ACKNOWLEDGMENTS

We thank T. Hollon and K. Miller for their help with frog video analysis. We appreciate the comments of Michael Owren and one anonymous reviewer that greatly improved the manuscript. This study was funded by NSF Grant No. IBN-0078150 and The University of Texas at Austin Cockrell School of Engineering.

[1]C. E. Shannon, "A mathematical theory of communication," Bell Syst. Tech. J. **27**, 379–423 (1948).
[2]W. W. L. Au, *The Sonar of Dolphins* (Springer-Verlag, New York, 1993).
[3]M. Hunter, Jr., A. Kacelnik, J. Roberts, and M. Vuillermoz, "Directionality of avian vocalizations: A laboratory study," Condor **88**, 371–375 (1986).
[4]A. Michelsen and P. Fonseca, "Spherical sound radiation patterns of singing grass cicadas, *Tympanistalna gastrica*," J. Comp. Physiol., A **186**, 163–168 (2000).
[5]K. Frommolt and A. Gebler, "Directionality of dog vocalizations," J. Acoust. Soc. Am. **116**, 561–565 (2004).
[6]H. Carl Gerhardt, "Sound pressure levels and radiation patterns of the vocalizations of some North American frogs and toads," J. Comp. Physiol., A **102**, 1–12 (1975).
[7]M. S. Dantzker, G. B. Deane, and J. W. Bradbury, "Directional acoustic radiation in the strut display of male sage grouse *Centrocercus urophasianus*," J. Exp. Biol. **202**, 2893–2909 (1999).
[8]M. Zuk and G. R. Kolluru, "Exploitation of sexual signals by predators and parasitoids," Q. Rev. Biol. **73**, 415–438 (1998).
[9]T. M. Peake, "Eavesdropping in communication networks," in *Animal Communication Networks*, edited by P. K. McGregor (Cambridge University Press, Cambridge, 2005), pp. 13–37.
[10]W. H. Cade, "Acoustically orienting parasites: Fly phonotaxis to cricket song," Science **190**, 1312–1313 (1975).
[11]S. Sakaluk and J. Belwood, "Gecko phonotaxis to cricket calling song: A case of satellite predation," Anim. Behav. **32**, 659–662 (1984).
[12]J. Bellwood and G. K. Morris, "Bat predation and its influence on calling behavior in neotropical katydids," Science **238**, 64–67 (1987).
[13]K. Schniederkötter and R. Lakes-Harlan, "Infection behavior of a parasitoid fly, *Emblemasoma auditrix*, and its host cicada *Okanagana rimosa*," J. Insect Sci. **4:36**, 1–7 (2004).
[14]G. R. Allen and J. Hunt, "Larval competition, adult fitness, and reproductive strategies in the acoustically orienting *Ormiine Homotrixa alleni* (Diptera: Tachinidae)," J. Insect Behav. **14**, 283–297 (2001).
[15]G. U. C. Lehmann, K.-G. Heller, and A. W. Lehmann, "Male bushcrickets favoured by parasitoid flies when acoustically more attractive for conspecific females (Orthoptera: Phanopteridae/Diptera: Tachinidae)," Entomol. Gen. **25**, 135–140 (2001).
[16]P. D. Bell, "Acoustic attraction of herons by crickets," J. New York Entomol. S. **87**, 126–127 (1979).
[17]M. D. Tuttle, L. K. Taft, and M. J. Ryan, "Acoustic location of calling frogs by *Philander opossums*," Biotropica **13**, 233–234 (1982).
[18]T. Halliday, *Sexual Strategy* (University of Chicago Press, Chicago, 1980).
[19]J. A. Endler, "Evolutionary implications of the interaction between animal signals and the environment," in *Animal Signals*, edited by Y. Espmark, T. Amudsen, and G. Rosenqvist (Tapir Academic, Trondheim, Norway, 2000).
[20]R. H. Wiley and D. G. Richards, "Adaptations for acoustic communication in birds: sound transmission and signal detection," in *Acoustic Communication in Birds*, edited by D. E. Kroodsma and E. H. Miller (Academic, New York, 1982), Vol. **1**.
[21]M. J. Ryan and N. M. Kime, "Selection on long-distance acoustic signals," in *Acoustic Communication*, edited by A. M. Simmons, A. N. Popper, and R. R. Fay (Springer, New York, 2003).
[22]M. J. Ryan, "The túngara frog," *A Study in Sexual Selection and Communication* (University of Chicago Press, Chicago, 1985).
[23]M. J. Ryan and A. S. Rand, "Mate recognition in túngara frogs: A review of some studies of brain, behavior, and evolution," Acta Zool. Sinica **49**, 713–726 (2003).
[24]M. Gridi-Papp, A. S. Rand, and M. J. Ryan, "Complex call production in túngara frogs," Nature (London) **441**, 38 (2006).
[25]M. D. Tuttle and M. J. Ryan, "Bat predation and the evolution of frog vocalizations in the Neotropics," Science **214**, 677–678 (1981).
[26]X. E. Bernal, A. S. Rand, and M. J. Ryan, "Acoustic preferences and localization performance of blood-sucking flies (*Corethrella* Coquillett)," Behav. Ecol. **17**, 709–715 (2006).
[27]X. E. Bernal, R. A. Page, A. S. Rand, and M. J. Ryan, "Cues for eavesdroppers: Do frog calls indicate prey density and quality?," Am. Nat. **169**, 412–415 (2007).
[28]K. S. Lynch, D. C. Crews, M. J. Ryan, and W. Wilczynski, "Hormonal state influences aspects of female mate choice in the túngara frog (*Physalaemus pustulosus*)," Horm. Behav. **49**, 450–457 (2006).
[29]M. J. Ryan and A. S. Rand, "Evoked vocal responses in male túngara frogs: Preexisting biases in male responses?," Anim. Behav. **56**, 1509–1516 (1998).
[30]O. Cramer, "The variation of the specific heat ratio and the speed of sound in air with temperature, pressure, humidity, and CO_2 concentration," J. Acoust. Soc. Am. **93**, 2510–2516 (1993).
[31]H. E. Bass, L. C. Sutherland, A. J. Zuckerwar, D. T. Blackstock, and D. M. Hester, "Atmospheric absorption of sound: Further developments," J. Acoust. Soc. Am. **97**, 680–683 (1995).
[32]A. Feng, P. Narins, C. Xu, W.-Y. Lin, Z.-L. Yu, Q. Qiu, Z.-M. Xu, and J.-X. Shen, "Ultrasonic communication in frogs," Nature (London) **440**, 333–336 (2006).
[33]D. Aylor, "Noise reduction by vegetation and ground," J. Acoust. Soc. Am. **51**, 197–205 (1972).
[34]W. T. Fitch, J. Neubauer, and H. Herzel, "Calls out of chaos: the adaptive significance of nonlinear phenomena in mammalian vocal production," Anim. Behav. **63**, 407–418 (2002).
[35]A. B. Pippard, "The driven anharmonic vibrator; subharmonics; stability," *The Physics of Vibration* (Cambridge University Press, Cambridge, 1978), Vol. **1**, Chap. 9.
[36]M. B. Hindmarsh and D. J. Jefferies, "On the motions of the offset impact oscillator," J. Phys. A **17**, 1791–1804 (1984).
[37]V. Tournat, V. E. Gusev, and B. Castagnède, "Subharmonics and noise excitation in transmission of acoustic wave through unconsolidated granular medium," Phys. Lett. A **326**, 340–348 (2004).
[38]L. E. Kinsler, A. R. Frey, A. B. Coppens, and J. V. Sanders, *Fundamentals*

of Acoustics, 3rd ed. (Wiley, New York, 1982).
[39]W. A. Watkins, E. R. Baylor, and A. T. Bowen, "The call of eleutherodactylus johnstonei, the whistling frog of bermuda," Copeia **1970**, 558–561 (1970).
[40]W. E. Duellman and L. Trueb, *Biology of Amphibians* (McGraw-Hill, New York, 1986).
[41]R. Dudley and A. S. Rand, "Sound production and vocal sac inflation in the túngara frog, Physalaemus pustulosus (Leptodactylidae)," Copeia **1991**, 460–470 (1991).
[42]A. S. Rand and R. Dudley, "Frogs in helium: The anuran vocal sac is not a cavity resonator," Physiol. Zool. **66**, 793–806 (1993).
[43]K. D. Wells, *The Ecology & Behavior of Amphibians* (The University of Chicago Press, Chicago, 2007).
[44]C. G. Don and A. J. Cramond, "Soil impedance measurements by an acoustic pulse technique," J. Acoust. Soc. Am. **77**, 1601–1609 (1985).
[45]D. T. Blackstock, *Fundamentals of Physical Acoustics* (Wiley, New York, 2000).